LA-UR-73-692

TITLE: Chemical Vapor Deposition of ZrC in Small Bore Carbon-Composite Tubes

AUTHOR(S): T. C. Wallace

SUBMITTED TO: For publication in the symposium volume on the Fourth International Conference on Chemical Vapor Deposition

los Alamos
scientific laboratory
of the University of California
LOS ALAMOS, NEW MEXICO 87544

MASTER

Form No. 836
St. No. 2629
1/73

UNITED STATES
ATOMIC ENERGY COMMISSION
CONTRACT W-7405-ENG. 36

CHEMICAL VAPOR DEPOSITION OF ZrC IN SMALL BORE CARBON-COMPOSITE TUBES*

Terry C. Wallace
Los Alamos Scientific Laboratory
P. O. Box 1663
Los Alamos, New Mexico 87544

ABSTRACT

Process conditions are described for the chemical vapor deposition of ZrC from the vapor phase consisting of zirconium tetrachloride, methane, hydrogen chloride, hydrogen and argon over the temperature range 1320 to 1775 K. From an analysis of the process conditions (initial composition of coating gas, axial temperature profile along the tubes, total pressure and length of deposition time), the subsequent ZrC coat thickness profiles and thermodynamic data, an equation expressing the variation of the axial rate of ZrC deposition is derived. This expression can be used for the estimation of process conditions required to yield a specified ZrC coat profile. Additionally, the variations of the chlorine and oxygen contents, the lattice parameter, the microstructure of the ZrC deposit and the coefficient of thermal expansion as a function of deposition temperature are described.

INTRODUCTION

Early in the Rover Program for the development of a graphite-based nuclear propulsion system which used hydrogen gas as the propellent, it was conclusively demonstrated that unprotected reactor components were severely attacked at the operating temperature. As a solution to this problem, Melvin G. Bowman of Los Alamos Scientific Laboratory developed the concept of the addition of a "protective gas" to the hydrogen propellant gas under operating conditions, such that the "protective gas" would react with the graphite-based components to form a protective carbide coating, but under conditions such that no deposition would occur on surfaces where free carbon was not available. One such group of protective gases investigated in 1957 included $TiCl_4(g)$, $ZrCl_4(g)$ and $NbCl_5(g)$ with varying amounts of $HCl(g)$. It was found that these additions in the presence of the hydrogen, would react with the exposed graphite surfaces to form the respective monocarbides, which served as protective coats. From these investigations a process was developed for diffusion controlled (carbon diffusion across the carbide layer) chemical vapor deposition of refractory carbides on graphite fuel elements.[1,2] It should be noted that Battelle Memorial Institute made an independent development of an equivalent

*Work performed under the auspices of the United States Atomic Energy Commission.

technique in 1957.[3] Even though these techniques yielded excellent coatings on unloaded graphite, it was not successfully used with UC_2 loaded graphite fuel elements until the latter part of 1961. From that point in time through December of 1972 some 46,000 fuel elements had protective boats applied by chemical vapor deposition at Los Alamos Scientific Laboratory.

NbC was the protective coating material used in the early years of the Program. As the operating criteria of the various nuclear propulsion systems became more stringent, it was necessary to improve the quality of the protective coats. The main direction that this effort took was the evolution of techniques for the deposition of NbC directly from the gas phase. This was accomplished by the addition of methane to the coating gas which eliminated the diffusion control aspects of the earlier process. These coats were much more adherent, but it was more difficult to control the coat thickness profile. With the development of composite fuel elements whose matrices were composed of mixtures of (U,Zr)C solid-solution carbide and graphite, it was necessary to develop techniques for the deposition of ZrC from the gas phase. During the last two years of the Program (1971 to 1972) an intensive effort was put into the analyses of the ZrC coating process to better understand the inter-relationships of the numerous coating process parameters.

The purpose of this paper is to:

- Describe the current process for chemical vapor deposition of ZrC on the surfaces of the bores of composite fuel elements.
- Describe the chemistry, physics, coat microstructure and kinetics of the deposition process.
- Present a model which describes the observed deposition rate in terms of the process parameters (initial coating gas composition, temperature profile down the fuel elements, total pressure of the system and time of deposition and fundamental thermodynamic properties.
- Summarize the performance of the ZrC protective coats.

EQUIPMENT

COATING FURNACE

Fig. 1 shows a perspective view of one of the coating furnaces used in this work. Power for the furnace is supplied by 200 kVA, 5 kHz. motor-generator set. Each motor-generator set is connected so that it

can be switched between either of two adjacent coating furnaces. This allows for greater versatility in that it is possible to cool in one furnace while the other is on a cooling cycle. The power from the motor-generator is connected to a coating furnace transformer which has a series of output taps ranging from 75 to 225 V in steps of 25 V. The induction coils are in three individual banks and by a simple switching arrangement, the voltage on any of these banks can be set by connecting with the output taps of the furnace transformer. Resonance in the system is provided by variable capacitor banks. The power system is interlocked with water flow and water temperature sensing devices to assure proper cooling of critical furnace components. Additionally there is a humidity sensor within the furnace shell to detect leaks from the cooling water channels. The inner most portion of the furnace is a graphite liner (14 in. diam, 1 in. thick and 86 in. long) surrounded by a graphite susceptor (16 in. diam, 1 in. thick and 85.75 in. long). Exterior to the susceptor is a 2 in. thick layer of Thermax insulation. The insulation is contained within 1 in. thick ceramic rings with 0.062$4$ in. thick sheet mica at the interface. In turn, the ceramic rings are supported by the water cooled, copper induction coils. The lower four sightports contain graphite tubes that pass through the furnace shell and terminate on the surface of the graphite liner. Ar is passed through these tubes so that the space between the liner and susceptor is continually purged of gaseous impurities. The flushing gas exits at the graphite support base and mixes with the effluent gas stream. The surface temperature of the liner is determined by optical pyrometry through these ports. They are positioned 12.5, 27.0, 41.5 and 56.0 in. relative to the inlet end of the positioned fuel elements. Periodically a temperature calibration is made between the surface temperatures measured at the sight port positions and simultaneous pyrometric readings vertically through the top sight port of the furnace to positioned steeped surfaces within the loading fixture. The calibrations are within ± 15° over a period of 3 months when the maximum operating temperature of the furnace is kept below 2200 K. The heat exchange baffle fits into the top of the loading fixture. The top sleeve fits into a 1 in. step joint on the top on the loading fixture. To assure that no furnace shell gases enter the coating gas stream at this point, a plenum is machined in the graphite line 8 in. above the joint. The plenum is connected through the second sight port to a differential pressure regulated Ar source that keeps the pressure in the plenum 15 torr above the coating gas stream pressure. As a consequence, the Ar flushes upward between the liner and the top sleeve, preventing furnace shell gases from entering this region. The graphite inlet tube screwed into the top sleeve is connected with a stainless steel inlet pipe through a clamped ball joint.

SALT VAPORIZER AND PROCESS GASES

$ZrCl_4(g)$ is supplied to the coating gas stream by a stainless steel vaporizer shown in Fig. 2. The vaporizer is suspended from a 250 lb load cell and suspended within an oven. The temperature of the

vaporizer and oven are sensed with thermocouples. In operation the oven temperature is kept at 600 K, and the temperature of the vaporizer is controlled (note the two pair of ring heaters at the top and bottom of the vaporizer body) between 600 to 630 K. The change in weight is monitored from the output of the load cell and displayed on an electronic scale.[4] The charge capacity of the vaporizer is approximately 90 lb. This unit is capable of sustaining a steady flow rate of 1 to 4 lb/h using the temperature dependence of the vapor pressure of $ZrCl_4$ for flow control. The delivery line from the valve at the top of the vaporizer body to the graphite inlet tube in the furnace is kept at 630 K to keep the gaseous salt from condensing. A warning device is incorporated into the circuit of the electronic scale so that an alarm can be activated if the delivery rate falls outside of a preset range.[5] The process gases (CH_4, HCl, H_2, Ar and HCl) are metered by calibrated Fischer-Porter Tri-Flat variable area flow meters. The gas pressure on the meter is fixed at 50 psi to assure accurate delivery. The metered gases are collected by a common manifold, heated to 600 K, mixed with the $ZrCl_4(g)$ and then piped into the furnace through a heated line. The differential pressure between the coating gas manifold and the ambient atmospheric pressure, as well as the differential pressure between the manifold and furnace shell, are monitored to detect malfunctions in the coating gas delivery system.

CONDENSING TRAP

At the base of the furnace the effluent gases are led to a water-cooled condensing trap. The purpose of the trap is to remove the fine aerosol of the unreacted zirconium halides that form upon cooling. A portion of the aerosol condenses within the trap body. At the end of the trap there is a fiber glass thimble which filters an additional portion of the aerosol. However, approximately 30% of the very fine particles pass on through. From the condensing trap the gases is passed through a water scrubber to remove the additional aerosol, HCl and any other water soluble gases. Next the gas is passed through a NaOH solution scrubber to remove any Cl_2 which may have been formed. Finally it is vented to the atmosphere through a 60 ft. stack.

COATING FIXTURE

One of the factors that makes this coating system versatile is the adaptability of the loading or coating fixtures for handling a wide range of part sizes and configurations. This system with a modification of the loading fixture described below was used for the development of a low density ZrC insulator.[6] Fig. 3 shows an end view of the coating fixture used in the bore coating work. Basically the body of the fixture is 12 in. diam. by 5.5 in. internal diam. and 50 in. long. The bottom of the fixture is fitted to a base (see Fig. 4) which collects the effluent gases from each element and conducts these gases to a common central exit plenum. Additionally the base has a bayonet socket for lifting the assembled unit from the loading cart and placement with-

in the coating furnace. Once the fixture is in place, the baffle assembly shown in Fig. 4 is fitted into the recessed area on the inner surface at the top of the coating fixture. The fuel elements are held in a vertical position from the adjustment sleeves shown in Fig. 3. The adjustment sleeves have a hexagonal interior cross section which makes a close fit with each element. Each element has been threaded on the inlet end to accept a graphite nut which keeps the element from falling through the sleeve and which makes a gas seal that forces the coating gases down through the bores.

MATERIALS

The materials used in the coating gas were purchased from commercial sources with the following specifications: $ZrCl_4$ - reactor grade, ≥ 99.5% pure with Hf ≤ 200 ppm; H_2 ≥ 99.9% pure; HCl ≥ 99.0% pure, extra dry; CH_4 ≥ 99.0% pure and Ar ≥ 99.995% pure.

The carbide-carbon composite fuel elements were fabricated at Los Alamos Scientific Laboratory. The fabrication details are available.[7] The fuel elements are 1.32 m long, have a hexagonal cross section with a flat to flat dimension of 19 mm, weigh approximately 1.1 kg and have a volume of $28 \cdot 10^{-6} m^3$. Each element has 19 heat exchange or coolant channels that run the full length of the element. The diameter of an individual coolant channel is 2.5 mm. Depending on the process conditions, the average coefficient of thermal expansion of the matrix material lies within the range 6.2 to 7.2 μm/m·K (average over the temperature range 293 to 2300 K). The ZrC protective coat is deposited in each coolant channel to a pre-specified profile. Additionally ZrC was deposited on the exterior surface and had a thickness of 38 to 50 μ. Fig. 5 shows the element cross section and the areas which were coated.

NON-DESTRUCTIVE MEASUREMENTS

A number of non-destructive testing techniques were developed by Group M-1 (Non-Destructive Testing) that were particularly useful in the evaluation of the ZrC coats. One such device was a β-back scatter probe. The sensing portion of the instrument consisted of a long probe (~ 75 mil dia) which could be inserted into the coated bores. A ^{90}Sr source and a detector were contained in the tip. The intensity of the β-particles back scattered to the detector is a function of the thickness of the ZrC coat at the position of the probe in the element. This technique offered a rapid means of determining the coat thickness profiles down individual bores. The instrument was limited to development runs where graphite elements were used. The HREC (high resolution eddy current) instrument was again a probe device which provided data on coat and matrix cracking along the length of a bore. The MULE (mass per

unit length examination) machine determined the mass per unit length along the element. It was based on the absorption of the radiation from a Co source by the mass of a segment of the fuel element interposed between the source and a detector. By making MULE measurements before and after a coating run it was possible to determine the quantity of ZrC deposited in the bores to an accuracy of 0.2%. This determined the ZrC coat profiles deposited on the composite fuel elements.

PROPERTIES OF CVD ZRC

The determination of the properties of a ZrC coat deposited in a 2.5 mm bore is a tedious undertaking. However, it was the pursuit of these property determinations which led to a better understanding of the interactions between the ZrC coat and the matrix.

IMPURITY CONTENT AS A FUNCTION OF DEPOSITION TEMPERATURE

The ZrC bore coats were sampled at fixed position along the axial length of a number of fuel elements from a number of different coating batches. These samples were analyzed for Cl, H, N and O. The N and H contents of the samples were invariably less than [illegible] ppm. There wasn't any significant variation with the sample location or coating batch. However, the Cl and to a lesser degree the O content always showed a decrease as the sampling position moved away from the inlet end of the fuel elements. When the sampling positions were correlated with the increasing temperature profile down the fuel element lengths for the different coating batches, it was found that the Cl and O content of the ZrC coats had a strong dependence on the deposition temperature. The results of these analyses are summarized in Table 1. Electron microprobe analyses across the ZrC coats indicated that the

TABLE 1. DEPENDENCE OF IMPURITY CONTENT AND LATTICE PARAMETER OF CVD ZrC AS A FUNCTION OF DEPOSITION TEMPERATURE

DEPOSITION TEMP, K	AVERAGE Wt% Cl	AVERAGE Wt% O	AVERAGE LATTICE PARAMETER, A
1400	1.2 ± 0.5	0.3 ± 0.1	4.706 ± 0.005
1450	0.5 ± 0.3	0.2 ± 0.1	4.701 ± 0.002
1500	0.15± 0.05	0.15± 0.10	4.699 ± 0.001
1550	0.10± 0.05	0.15± 0.10	4.6983± 0.0005
1600	0.05± 0.05	0.15± 0.10	4.6983± 0.0005

C/Zr ratio was essentially 1. Segments of the fuel elements heated for several h some 500° above their deposition temperatures in an Ar atmosphere showed a decrease in the Cl (factor of 1/2 to 1/3) and O (10 to 50%) contents.

X-RAY LATTICE PARAMETER AS A FUNCTION OF DEPOSITION TEMPERATURE

Concurrent with the above sampling, x-ray samples were also taken. It was found that the lattice parameter of the CVD ZrC had a strong dependence on the deposition temperature. The lattice parameter decreased as the deposition temperature increased. The results are given in Table 1. Since it is known that dissolved oxygen lowers the ZrC lattice parameter,[8] it would appear that the Cl is in the ZrC lattice and causes an increase in the lattice parameter. Heat treatment, as above, results in a lowering of the lattice parameter.

THERMAL EXPANSION OF CVD ZrC

The mismatch between the coefficients of thermal expansion (CTE) of the ZrC coat and the matrix leads to an induced strain in the coat when their temperature differs from the deposition temperature. In a series of experiments the CTE was measured on tubes of ZrC (13 cm long 13.5 mm dia. and wall thickness of 1.0 to 1.3 mm) which had been fabricated by the CVD process. Those tubes which had been deposited at ~1615 K (low chlorine content) had repeatable expansion characteristics (± 1%) when cycled to 2300 K two times. The CTE of these tubes (293-2300 K) was 7.67 μm/m·K. From this value and that quoted earlier for the composite fuel elements it is apparent that upon cool down from the coating temperature, the coat will be in strain. It was found that for 50-100 μ thick coats that cracking always occurred in the bores when the induced cool down strain exceeded 1000 μm/m. This observation lead to the requirement that the matrix should have as high of a CTE value as possible. However, it was found that a CTE value of 7.0 μm/m·K was about the maximum that could be achieved. Additionally it should be noted that temperature gradients (present under reactor operating conditions) across the coat-matrix interface could also induce a strain. The maximum value that occurred under hot test conditions were of the order of 700 μm/m. The CTE determination on the tubes that had 0.5 to 1.5 % Cl showed a very erratic behavior at temperatures above their deposition temperature indicating dimensional instability. However, once they had been heated to 2300 K three successive times, their expansion properties were well behaved and reproducible. When the coat and matrix are heated above the deposition temperature the coat is in compression. At temperatures > 2300 K creep and grain growth occur in a few minutes at the coat-matrix interface. See Fig. 6. Once the strain has been relieved, the coat-matrix interface acts as if the deposition had been at the test temperature and a larger strain is induced on this cool down than on the original coating cool down. It was believed that if the deposition temperature was increased the dimensional stability of the coat (and perhaps its strength would be increased, and that the amount of creep would be diminished resulting in fewer cracks forming upon cool down from reactor operating temperatures.

MICROSTRUCTURE OF CVD ZrC

The photomicrograph in Fig. 7 shows the typical microstructure of a ZrC coat deposited at ~ 1400 K. At the matrix-coat interface the microstructure invariably shows fine, equiaxed grains. From this region to the gas-coat interface columnar crystal grains are observed. The length of the crystal grains are nearly equal to the ZrC layer thickness. As the deposition temperature is increased, the emergent angle of the columnar grains widens. Fig. 8 shows the microstructure of a coat deposited at 1600 K. When the deposition temperature rises above 1600 K there have been occassions when preferred growth cones formed. Fig. 9 shows the microstructure of a preferred growth cone. Figs. 10a and 10b show the surface morphology and coated coolant channel cross section of an element in which cone growth was rather severe. The protrusion of these cones into the coolant channels causes turbulence in the hydrogen gas stream under reactor operating conditions which causes an unduly large pressure drop. It has been observed that the frequency of these cones vary from bore to bore in a given element. As a consequence there is an unequal flow of hydrogen down the bores which results in abnormally large temperature gradients. Such a condition is unacceptable. The growth of these cones could be eliminated by careful control of the process parameters (temperature profile and initial coating gas concentration).

PROCESS ANALYSIS AND RESULTS

As the requirement developed for rapid evaluation of a number of diverse processing parameter changes (ie, higher deposition temperatures and wide range of initial coating gas compositions) it became apparent that an intensive analysis of the relationship between the process parameters of the coating system and the resultant coat profiles was needed. It was expected that the analysis would lead to a better understanding of the fundamentals of the deposition process and also lead to a mathematical model which could be used for computer simulation of coating runs under a wide range of parameter changes. In the long run this would save considerable material costs and time.

THERMODYNAMIC FUNDAMENTALS OF DEPOSITION PROCESS

The overall deposition reaction may be represented by the equation

$$ZrCl_4(g) + CH_4(g) = ZrC(s) + 4HCl(g) \qquad (1)$$

This thermodynamic relation not only establishes the lower bound for the coating gas composition, but also serves as the basis for mass balance calculation along the axial length of the fuel elements. It also suggests that the partial pressure of $HCl(g)$ will have a strong effect on the deposition rate. As a consequence one must also consider the reduction of $ZrCl_4(g)$ in the system.

$$ZrCl_4(g) + \tfrac{1}{2}H_2(g) = ZrCl_3(g) + HCl(g) \qquad (2)$$

$$ZrCl_3(g) + \tfrac{1}{2}H_2(g) = ZrCl_2(g) + HCl(g) \qquad (3)$$

The reduction reaction is important near the coating gas inlet end of the elements because it determines the quantity of HCl formed which strongly influences the initial deposition rate. The quantities which have an effect on the deposition and which can be calculated from the above thermodynamic relations and appropriate mass balance equations as function of axial position along the element are: P_{Salt}-sum of the partial pressures of the $ZrCl_4(g)$, $ZrCl_3(g)$ and $ZrCl_2(g)$, P_{CH_4}-partial pressure of methane, P_{HCl}- partial pressure of hydrogen chloride and P_{H_2}- partial pressure of hydrogen.

COMPUTATIONAL SCHEME

Measured Process Parameters. The metered flows of the process gases and $ZrCl_4(g)$ (at STP) along with the measurement of the total pressure in the coating system fixes the initial molar flow rates of the components of the coating gas. The weight gain on the baffle and top lid assemblies along with the length of time the coating gases on determines the molar deposition rate in that region. The average temperatures determined at the four sight ports establishes the temperature profile along the elements. After a coating run is completed, the total weight gain of the elements, the MULE data and the β-back scatter coat thickness data affords a determination of the mass and coat thickness profiles. Since the deposition process is observed to be linear with time, one also has a measure of the molar and coat thickness deposition rates as a function of axial position along the fuel elements.

Calculated Process Parameters. The continum of reactions that occurs in the bores is approximated by dividing the element into 10 equal segments and proceeding with the following iterative computations. Starting with the first segment at the inlet end, there are two reactions that must be taken into account. The first is the calculation of the total change that has occurred in the gas stream due to the prior deposition of ZrC. For this calculation one assumes that depletion of $ZrCl_4(g)$ and $CH_4(g)$ and generation of $HCl(g)$ are directly proportional to the sum of the weight of ZrC that has been deposited in the sleeve and baffle region plus 1/2 of the amount deposited in the first segment of the fuel elements. Using Eq. (2) for the molar balance relations the total pressure and individual flow rates, one can compute the average partial pressures of the coating gas constituents. The second reaction that must be taken into account is the partial reduction of $ZrCl_4(g)$. The new equilibrium partial pressures of the coating gas constituents can be found from the solution of the following 5 simultaneous equations:

$$P_{Salt} = P_{ZrCl_4} + P_{ZrCl_3} + P_{ZrCl_2} \quad (4)$$

$$P_{H_2} = P^o_{H_2} - \tfrac{1}{2}P_{ZrCl_3} - P_{ZrCl_2} \quad (5)$$

$$P_{HCl} = P^o_{HCl} + P_{ZrCl_3} + 2P_{ZrCl_2} \quad (6)$$

$$K_1 = P_{ZrCl_3} \cdot P_{HCl} / P_{ZrCl_4} \cdot P^{\frac{1}{2}}_{H_2} \quad (7)$$

$$K_2 = P_{ZrCl_2} \cdot P_{HCl} / P_{ZrCl_3} \cdot P^{\frac{1}{2}}_{H_2} \quad (8)$$

where P_{Salt}, $P^o_{H_2}$, and P^o_{HCl} are the values calculated from the first reaction. K_1 and K_2 are calculated from the thermodynamic data for Eqs. (2) and (3) and the interpolated temperature at the mid point of the segment. Finally the average stoichiometry of the zirconium halides was computed for the midpoint, ie

$$n = (4 \cdot P_{ZrCl_4} + 3P_{ZrCl_3} + 2P_{ZrCl_2})/P_{Salt} \quad (9)$$

The above interative computation is repeated for each successive segment taking into account all prior deposition plus $\frac{1}{2}$ of the amount that occurred in the segment of interest. As a result of these series of computations a set of data is generated for each particular coating run which contains the deposition rate, R(μ/h), the partial pressures of the coating gas constituents, the average composition of the halide, $ZrCl_n$, and the deposition temperature for specified segments along the fuel element lengths.

RESULTS OF ANALYSIS

Analysis of the data for 20 coating runs over a wide range of process parameters lead to the following expression for the deposition rate

$$R = (P_{Salt} \cdot P_{CH_4} \cdot P^{\frac{1}{2}(n-2)}_{H} / P^n_{HCl}) \; A \exp(-B/T) \quad (10)$$

where $A = (4.8 \pm 1.8) \cdot 10^{22}$ and $B = 86{,}120 \pm 870$. To give a graphical presentation of the degree to which Eq. (10) represents the coating data, the quantity

$$R \cdot P^n_{HCl} / (P_{Salt} \cdot P_{CH_4} \cdot P^{\frac{1}{2}(n-2)}_{H_2})$$

is plotted versus 1/T,K for the 20 coating runs in Fig. 11. The above rate equation suggests that the rate determining step is the reaction of the zirconium halide with the surface, ie

$$ZrCl_n(g) + n/2\ H_2(g) = (Zr)_{surface} + n\ HCl(g) \quad (11)$$

Ultimately Eq. (10) was incorporated into a computer program which could be used reliably to simulate diverse coating runs and was instrumental in the development of the high temperature ZrC coating process. Table 2 gives the process conditions for a high temperature ZrC

protective coat. These are the conditions used to coat the elements which gave the best performance (see Table 3).

TABLE 2. PROCESS CONDITION FOR THE DEPOSITION OF A HIGH TEMPERATURE ZrC COAT IN THE BORES OF A COMPOSITE FUEL ELEMENT

INITIAL COMPOSITION OF COATING GAS[a] CONSTITUENTS	FLOW (STP)	DIST. FROM INLET END cm	COAT DEPOSITION TEMPERATURE, K	FINAL COAT THICKNESS, μ
$ZrCl_4$	1.4 l/min	12.7	1525	60
CH_4	1.0 l/min	25.4	1540	89
H_2	75.0 l/min	50.8	1580	119
Ar	75.0 l/min	76.2	1615	132
HCl (1^{st} 20 h)	3.0	101.2	1640	135
HCl (last 5h)	0.0	127.0	1660	132

[a] The coating time was 25 h and the average pressure in the coating system was 0.88 atm. This flow of gas was used to coat 18 element simultaneously.

SUMMARY OF PERFORMANCE OF ZrC PROTECTIVE COATS

One of the goals of the Rover Program was to develop a composite fuel element which would operate at a high temperature with a minimum of carbon loss. This goal was achieved in part by the development of process conditions for the application of ZrC protective coats at high deposition temperatures. Table 3 shows the improvement that was made

TABLE 3. DEPENDENCE OF MASS LOSS RATE (HOT GAS TEST[a]) OF COMPOSITE FUEL ELEMENTS[b] WITH ZrC PROTECTIVE COATS (130 thick) ON THE PROTECTIVE COAT DEPOSITION TEMPERATURE

COAT DEPOSITION TEMPERATURE, K	TEMPERATURE OF COAT IN TEST, K	MASS LOSS RATE[c] (g/cm-s)
1400	2750	failure
1500	2750	$13 \cdot 10^{-5}$
1650	2750	$4 \cdot 10^{-5}$

[a] Element was electrically heated. The flow rate of H_2 down the 19 coolant channels was 23.3 g/s.

[b] The CTE of the composite elements was 6.8 μm/m·K.

[c] The mass loss rate was determined by dividing the weight of the carbon lost from the test segment (1 cm) of the fuel element by the time of the test.

over the last two years in relation to the effect of coat deposition temperature on hot gas test performance.

//

ACKNOWLEDGEMENTS

The success of any undertaking is dependent to a large degree on the interest and inspiration of ones co-workers. In particular I would like to acknowledge that it was Dr. Melvin G. Bowman's pioneering efforts and leadership that led to the establishment of a Rover fuel element coating facility at Los Alamos Scientific Laboratory. I would also like to acknowledge the stimulation and help given by the Rover Fuel Element Committee: L. L. Lyon and A. R. Driesner, formerly Group N-1 (Materials); J. C. Rowley, formerly Group N-7 (Analyses); K. V. Davidson, Group CMB-6 (Materials Technology); R. J. Bard, Group CMB-8 (Physical Chemistry and Metallurgy); and H. J. Fullbright, Group M-1 (Non-Destructive Testing). The administrative and technical guidance of J. D. Farr, Group CMB-3 (High Temperature Chemistry) is also gratefully acknowledged.

REFERENCES

1. MELVIN G. BOWMAN, "Refractory Carbides as Protective Coatings on Graphite Fuel Elements," Proceedings of Nuclear Propulsion Conference, Naval Postgraduate School, Monterey, California, August 15-17, 1962. AEC Research and Development Report, TID-7653 (Pt. II), p. 378-381. Formerly classified CRD, now unclassified.

2. D. C. WINBURN and R. K. MONEY, "Protective Coating Technology for Kiwi Fuel Elements," p. 394-403, ibid.

3. J. M. BLOCHER, Jr., C. J. ISH, D. P. LEITER, Jr., L. F. PLOCK and I. E. CAMBELL, "Carbide Coatings on Graphite," BMI-1200, June 28, 1957. Batelle Memorial Institute, Columbus, Ohio.

4. GEORGE N. RUPERT, "Electronic Scale for Measuring Mass Flow," Los Alamos Scientific Laboratory Report LA-3659 (March, 1967).

5. GEORGE N. RUPERT and T. C. WALLACE, "Instrumentation for High Temperature Chemical Process Control," Los Alamos Scientific Laboratory Report LA-5186-MS, Pts. I and II, (February 1973).

6. ALLEN R. DRIESNER, EDMUND K. STORMS, PAUL WAGNER and T. C. WALLACE, "High Temperature-Low Density ZrC Insulators Made by Chemical Vapor Deposition," Fourth International Conference on Chemical Vapor Deposition, October 7-12, 1973, Boston, Massachusetts.

7. K. V. DAVIDSON, W. W. MARTIN, D. H. SCHELL, J. M. TAUB and J. W. TAYLOR, "Development of Carbide-Carbon Composite Fuel Elements for Rover Reactors," Los Alamos Scientific Laboratory Report LA-5005, October 1972. Formerly Classified CRD, now unclassified.

8. EDMUND K. STORMS, The Refractory Carbides, Academic Press, New York and London (1967).

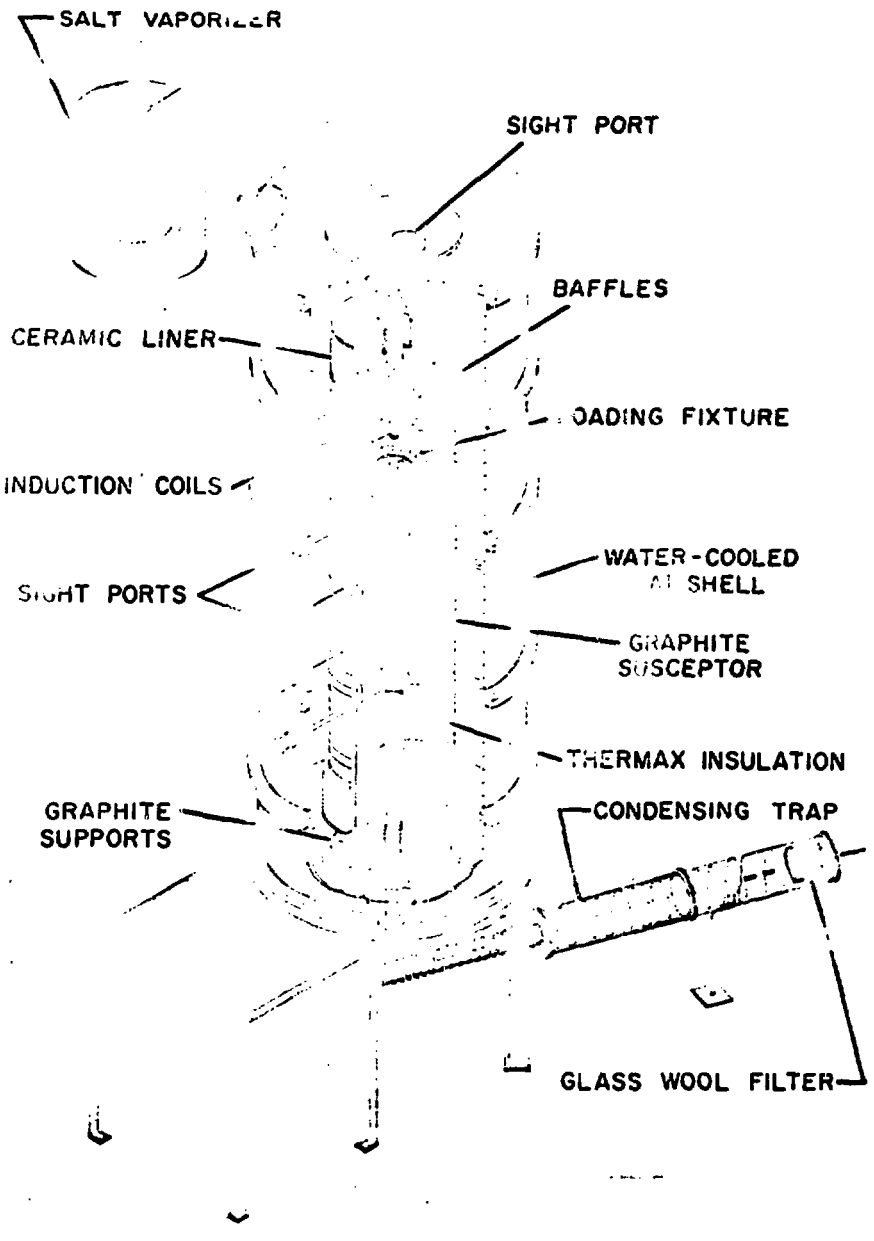

FIGURE 1. PERSPECTIVE VIEW OF ZrC COATING FURNACE.

FIGURE 2. $ZrCl_4$ VAPORIZER UNIT.

FIGURE 3. END VIEW OF LOADING FIXTURE.

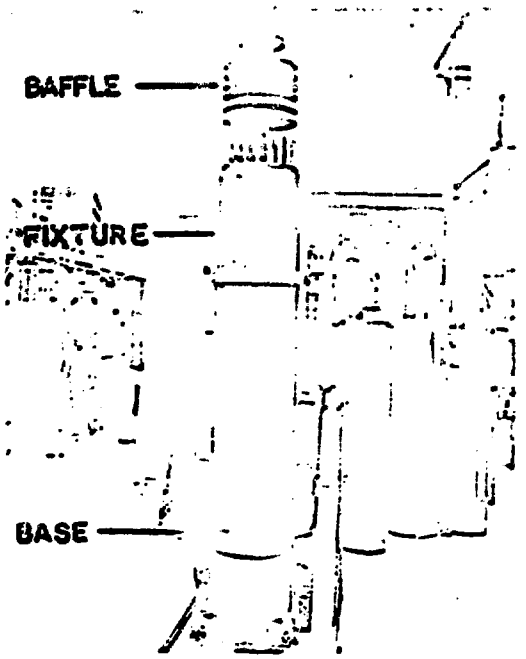

FIGURE 4. VIEW OF LOADING FIXTURE, BASE AND BAFFLE ASSEMBLY.

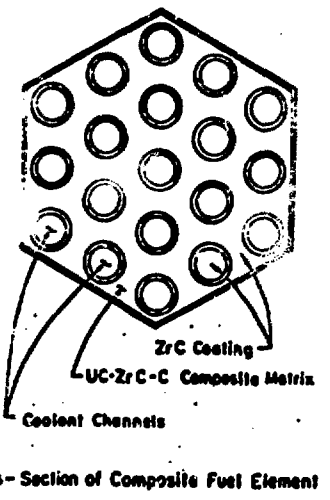

FIGURE 5. CROSS SECTION OF FUEL ELEMENT.

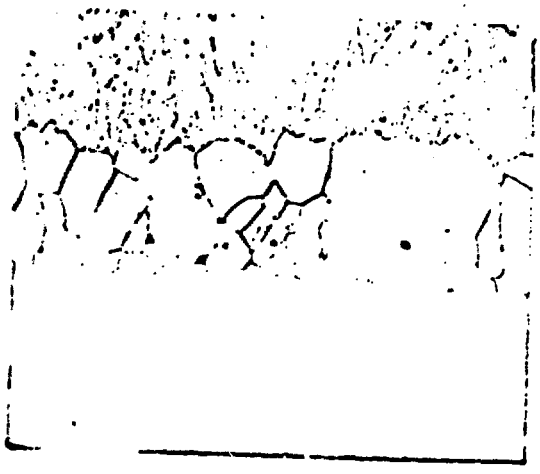

FIGURE 6. PHOTOMICROGRAPH OF GRAIN GROWTH THAT OCCURS AT THE COAT-MATRIX INTERFACE AT 2300 K.

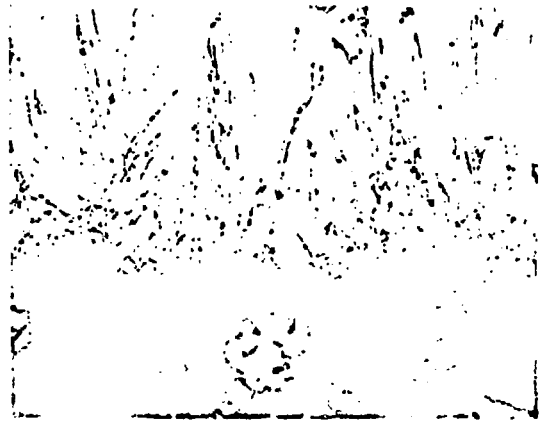

FIGURE 7. MICROSTRUCTURE OF ZrC COAT DEPOSITED AT 1400 K.

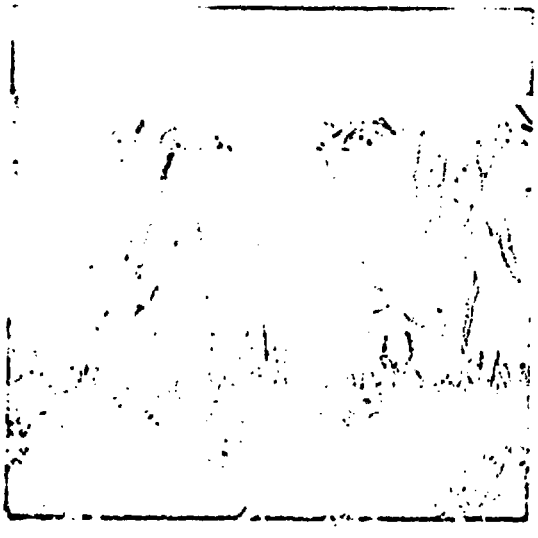

FIGURE 8. MICROSTRUCTURE OF ZrC COAT DEPOSITED AT 1600 K.

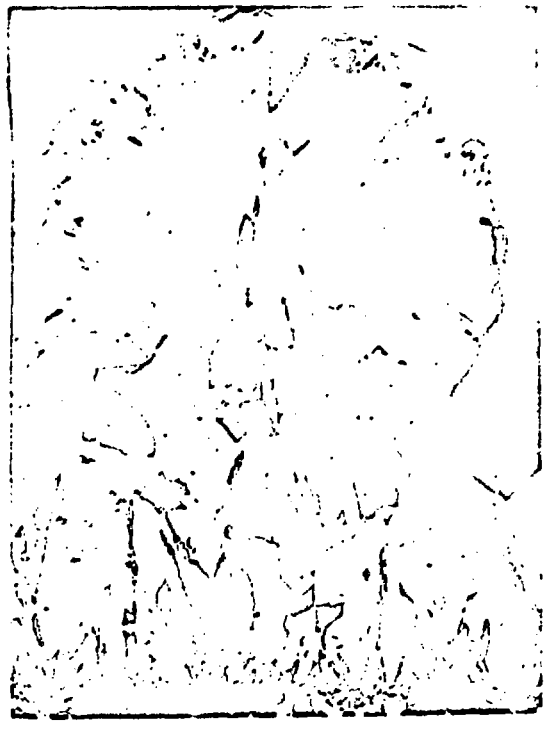

FIGURE 9. MICROSTRUCTURE OF PREFERRED GROWTH CONE. DEPOSITION TEMPERATURE 1700 K.

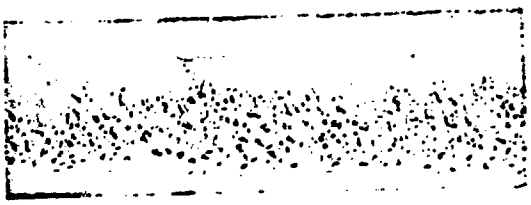

FIGURE 10a. SURFACE MORPHOLOGY OF PREFERRED GROWTH CONES.

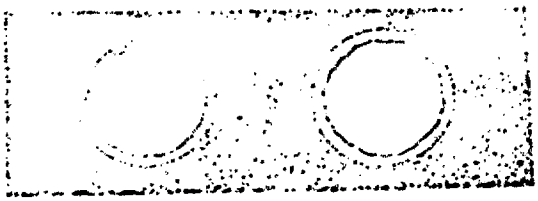

FIGURE 10b. CROSS SECTION OF COOLANT CHANNEL WITH PREFERRED GROWTH CONES.

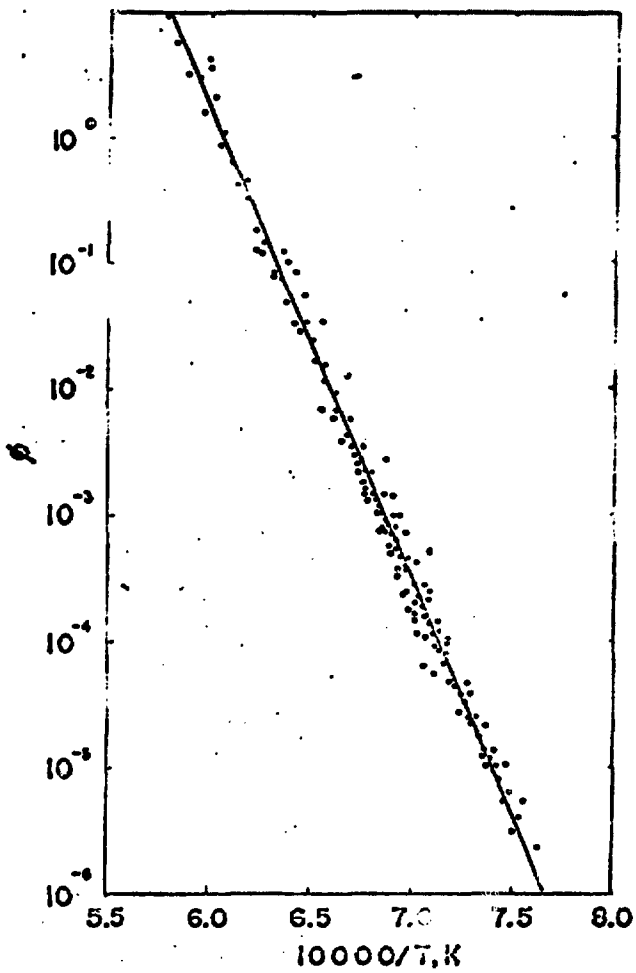

FIGURE 11. PLOT OF $\phi = R \cdot P_{HCl}^{n} / (P_{Salt} \cdot P_{CH_4} \cdot P_{H_2}^{(n-2)})$ VERSUS THE RECIPOCAL TEMPERATURE, 1/K. THE LINE REPRESENTS THE EQUATION, $\phi = A \cdot \exp(-B/T)$, WHERE A AND B ARE GIVEN BY EQ. 10.

INDEX	PAGE